Available online at www.sciencedirect.com
ScienceDirect
Energy Conversion and Management 49 (2008) 832–842
ENERGY CONVERSION & MANAGEMENT
www.elsevier.com/locate/enconman

Equilibrium modeling of global reduction reactions for a downdraft (biomass) gasifier

Avdhesh Kr. Sharma *

Department of Mechanical Engineering, Deen Bandhu Chhotu Ram University of Science and Technology, Murthal, Haryana 131 039, India

Received 28 November 2006; accepted 29 June 2007
Available online 17 August 2007

Abstract

This article proposed a full equilibrium model of global reduction reactions for a downdraft biomass gasifier in order to predict the accurate distribution of various gas species, unconverted char and reaction temperature. Full equilibrium of the global reduction reactions has been described using thermodynamics principles based on the stoichiometric approach. Model predictions for equilibrium constants for reduction reactions and dry gas composition have been validated by comparing the data collected from various sources. Simulations modeling the influences of moisture content in feedstocks, pressure, equivalence ratio and initial temperature input on dry gas composition, unconverted char, calorific value of gas, gasification efficiency, outlet gas temperature and endothermic heat released in char bed. For optimal energy conversion of Douglas fir bark, the range of moisture content and equivalence ratio should be limited to 10–20% and 0.3–0.45 respectively, while the initial temperature in the reduction reaction zone should not be less than 1200 K. The accuracy of the prediction of the equilibrium model depends on the correctness of the initial conditions of temperature and reactants concentrations.

Keywords: Modeling; Chemical equilibrium; Downdraft gasifier; Producer gas; Reduction reactions

1. Introduction

Biomass gasification has emerged as a very promising technology to fulfill the need of a decentralized quality power supply to remote rural areas. Here, biomass undergoes a series of thermochemical processes in a gasifier under a restricted supply of the air or oxygen in order to generate a combustible gaseous mixture such as CO, H_2 and CH_4. The primary goal of biomass gasification is optimal energy conversion of the solid biomass into a combustible gaseous product known as producer gas. In a gasifier, the reaction temperature controls the reaction rates and the directions of various reactions and, hence, the efficiency of thermochemical conversion. Thus, understanding the chemistry of reactions in a downdraft biomass gasifier is essential in order to optimize the quality and quantity of the final gas.

Recent theoretical studies include kinetic or non-equilibrium modeling of the reduction reactions of a downdraft biomass gasifier [1–3]. These models describe the char reduction process using kinetic rate expressions obtained from experiments and permit better simulation of the experimental data where the residence time of gas and biomass is relatively short. The kinetic model of Wang and Kinoshita [1] is based on a mechanism of surface reactions in the reduction zone assuming a given residence time and reaction temperature, while Giltrap et al. [2] assigned a constant value of char reactivity factor and adopted the kinetics rate expressions of Wang and Kinoshita [1] in their model to predict the gas concentration and reaction temperature along the char reduction zone of a downdraft gasifier. Babu and Sheth [3] suggested an exponentially varying char reactivity factor in order to predict better simulation of temperature profile in the reduction reaction

* Tel.: +91 130 2484085; fax: +91 130 2484003.
E-mail address: avdhesh_sharma35@yahoo.co.in

0196-8904/$ - see front matter © 2007 Elsevier Ltd. All rights reserved.
doi:10.1016/j.enconman.2007.06.025

Nomenclature

A	cross sectional area of reactor
C_p	specific heat (kJ/kg K)
dL	length of CV
$\bar{g}_i^0$	Gibbs function of ith constituent (kJ/kmol)
k	thermal conductivity (W/m K)
k_{eff}	effective thermal conductivity of char bed (W/m k)
$\dot{n}$	molar flow rate
$\dot{Q}_{\text{reac}}$	heat absorbed in reduction zone (kW)
R	universal gas constant (kJ/kmol K)
T	temperature (K)
Y	mass fraction for each species
Ag–Gg	constants in Eq. (12)
CV	control volume
d_{b}	initial particle diameter
ΔG_j°	Gibbs function changes for jth reaction (kJ)
$K_{\text{eq},j}$	equil constants, jth reaction
$\dot{m}$	mass flow rate (kg/s)
mw	molecular weight
P	pressure (N/m^2)
$\dot{Q}_{\text{loss}}$	heat loss to surroundings (kW)
Sg_{char}	sp. gravity
T_{A}	ambient temperature (K)
$\dot{w}$	molar flow rate due to moisture in feedstock

Greek letters

$\dot{\wp}$	molar flow rate of O_2 for gasification
χ	mole fraction of each species

Subscripts/Superscripts

HB	H atoms in C_6 chemical formula of biomass React reactants
OB	O atoms in C_6 chemical formula of biomass Prod products
C/char	char

zone. They have also compared the role of constant, linearly varying and exponentially varying char reactivity factors on the model predictions.

On the other hand, equilibrium models are also important in order to predict the thermodynamic limits of chemical reactions describing the gasification process. For downdraft gasifier designs, however, both pyrolysis and gasification products are forced through the hottest zone (oxidation zone) so that equilibrium is established after a relatively brief time period [4]. Recent modeling efforts include the application of chemical equilibrium modeling for biomass gasification [5–9]. Among these models, Ruggiero and Manfrida [5] developed a simple model for biomass gasification considering the Gibbs free energy of reaction and emphasized the potential of an equilibrium model. The models of Zainal et al. [6] describe the equilibrium composition using water–gas shift and methane–char reactions. The predictions of Zainal et al. [6] highlight the effect of moisture content in wood chips and the reaction temperature on gas composition for a given bed temperature using different biomass materials. Ruggiero and Manfrida [5] and Zainal et al. [6] have confirmed that the residence time of the reactants can be considered to be high enough to reach chemical equilibrium. Altafini et al. [7] and Malgar et al. [8] reported a similar conclusion regarding the influence of air/fuel ratio in addition to biomass moisture content on adiabatic temperature, gas composition and efficiencies. Prins et al. [9] describe the gasification systems using chemical equilibrium and reported that the equilibrium model presents the highest gasification efficiency that can be possibly attained for a given fuel.

From the exhaustive review, It is observed that most of the stoichiometric equilibrium models of biomass gasification developed in the past describe the equilibria of reduction reactions, viz. methane–carbon reaction (heterogeneous reaction) and water gas shift reaction (homogeneous reaction) assuming: (1) the drying, pyrolysis and gasification processes are lumped together in a single zone, (2) residence time for reactants is sufficiently high in order to establish chemical equilibrium and (3) all the carbon is gasified. In the present article, therefore, full equilibrium modeling of the global reduction reactions for char–gas and gas–gas reactions in the reduction zone of the downdraft biomass gasifier has been presented. The proposed model also presents the unconverted char yields, eliminating assumption (3) as discussed above. The energy equation has been modeled to account for the thermal interactions of neighboring zones and the surroundings in order to predict accurate reaction temperatures in the char bed. The model predictions for species composition are found in reasonable agreement with data collected from various sources for downdraft biomass gasifiers.

2. Physical description

In fixed bed gasifiers, the distributions of reaction regions or zones are different depending on the type of gasifier designs. For downdraft designs, Graboski and Bain [10] and Reed and Markson [11] reported that pyrolysis and combustion occur simultaneously, while for updraft designs, the pyrolysis, oxidation and reduction reactions take place in separate regions as shown in Fig. 1. For I.C. engines application, downdraft designs are usually employed, as these designs are known to provide relatively tar free or clean gases. Here, biomass and air enter from the open top and approach the comparatively high temperature zone. Thermal decomposition dominates progressively as the temperature increases, yielding char and volatiles.

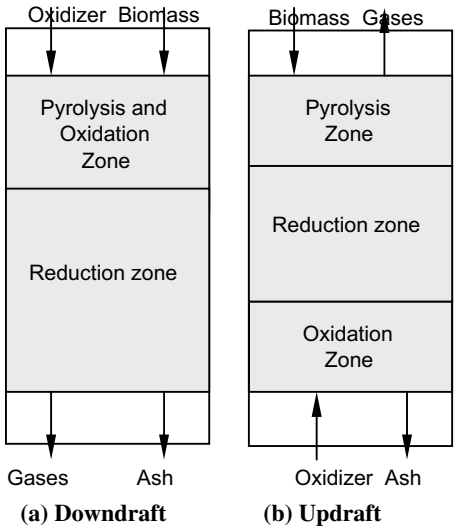

Fig. 1. Zonal description of the gasifier [10].

With the availability of air, these combustible products get ignited and provide the exothermic reactions to enhance further pyrolysis and also thermal cracking of the pyrolysis products into lower molecular weight components. For the present work, the whole process of biomass drying, pyrolysis and combustion of volatiles due to the presence of air has been described in the flaming pyrolysis zone. As the volatiles deplete, the combustion process start receding, and finally, the flames die down leading to char reduction with a glowing surface [11,12]; these chemical reactions are being described in the char reduction reaction zone. For model development, the following assumptions are invoked:

1. Reaction temperature and residence time for reactants are sufficiently high to reach chemical equilibrium.
2. The fuel bed is isotropic and the solid particles are spherical with uniform diameter.
3. Solid and gases are in thermal equilibrium.
4. Gases are assumed to behave ideally.

3. Model formulation

3.1. Initial conditions

In order to obtain the concentration of species as input information to the reduction reaction model of the downdraft gasifier; the drying is considered to occur instantaneously, while the pyrolysis and oxidation process can be described simultaneously in a flaming pyrolysis zone. Thus, the process of drying, pyrolysis and oxidation can be considered an open system, which can be described using a single reaction as

$$\begin{aligned} &C_6H_{HB}O_{OB}N_{NB}S_{SB} + \dot{w}H_2O + \dot{\varphi}O_2 + 3.76\dot{\varphi}N_2 \\ &= \dot{n}_{CO}CO + \dot{n}_{CO_2}CO_2 + \dot{n}_{H_2}H_2 + \dot{n}_{H_2O}H_2O \\ &\quad + \dot{n}_{CH_4}CH_4 + \dot{n}_{C}C + \dot{n}_{N_2}N_2 + \dot{n}_{SO_2}SO_2 \end{aligned} \quad (1)$$

Here, $C_6H_{HB}O_{OB}N_{NB}S_{SB}$ is the chemical formula of dry biomass, $\dot{w}$ denotes the molar flow rate of moisture in the feedstock and $\dot{\varphi}$ represents the oxygen moles in the atmospheric air (which is a function of equivalence ratio). The subscripts in the chemical formula of biomass as HB, OB, NB and SB can be obtained from ultimate analysis of the biomass. $\dot{n}$ denotes the molar flow rate of each species in the product gas per mole of dry biomass.

Char yield can be known from proximate analysis. Shafizadeh [13] reported that the hydrogen and oxygen content in the char decreases sharply as the temperature increases, thus, char can be assumed to be pure carbon. If the equivalence ratio, biomass composition, moisture content in the biomass fuel and char yield has been supplied as input, the unknowns in Eq. (1) can be related using elemental balance equations for C, H, O, N and S, respectively. Two more relations would be needed to close the system. The approximation of Wang and Kinoshita [1] as a function of the formation ratio of water vapour to carbon dioxide ($\lambda = 1$) has been employed in the present work

$$\dot{n}_{H_2O} = \lambda \dot{n}_{CO_2} + \dot{w} \quad (2)$$

For the other relation, Wang and Kinoshita [1] have assumed the initial concentrations of hydrogen and carbon monoxide in the reduction zone can be neglected at the elevated oxidation temperatures. When the present work used these approximations, it resulted in unrealistically low reaction temperatures in the reduction zone. Therefore, in the present work, the latter approximation has been dropped and replaced by a more realistic approximation as

$$\dot{n}_{H_2} = \gamma \dot{n}_{CO} \quad (3)$$

Here, γ is the hydrogen to carbon dioxide formation ratio. In the present work, γ is fixed at 1.0. These concentrations of oxidized products can serve as the initial concentrations of the reactants for the reduction zone.

3.2. Modelling reduction reactions

The reduction zone chemistry has been described by five global reduction reactions (R1–R5) to predict the concentrations of seven gaseous species (i.e. CO, CO_2, H_2, H_2O, CH_4, N_2 and SO_2) and unconverted char (if any). Here, char is consumed gradually in the complete absence of oxygen due to the homogeneous and heterogeneous reactions listed below

$$\text{R1 : Water gas shift reaction} \quad : CO + H_2O \overset{\in_1}{\leftrightarrow} CO_2 + H_2$$

$$\text{R2 : Steam reforming reaction} \quad : CH_4 + H_2O \overset{\in_2}{\leftrightarrow} CO + 3H_2$$

$$\text{R3 : Boudouard reaction} \quad : C + CO_2 \overset{\in_3}{\leftrightarrow} 2CO$$

$$\text{R4 : Water gas (primary) reaction} \quad : C + H_2O \overset{\in_4}{\leftrightarrow} CO + H_2$$

$$\text{R5 : Methanation reaction} \quad : C + 2H_2 \overset{\in_5}{\leftrightarrow} CH_4$$

Here, $\in_j$ is the degree of advancement of the jth reaction in the system. It can be treated as positive if the reaction pro-

ceeds in the forward direction, otherwise it is negative. All gaseous products present in the system are assumed to behave ideally. N_2 and SO_2 are considered to be inert in the reduction environment.

For the stoichiometric equilibrium approach, it is necessary to select the set of chemical reactions to describe the system. Once the set of reactions are selected, the mass balance for each reaction can be expressed in terms of compact notation as

$$\sum_{i=1}^{\mathrm{ns}} Sr_{j,i}A_i = \sum_{i=1}^{\mathrm{ns}} Sp_{j,i}A_i \quad \text{for } j = 1, 2, \ldots R_n \tag{4}$$

Here, ns denotes the number of species in the system including solid char. A_i represents the chemical formula of each species in the system such as $A_i = \mathrm{CO}$, $\mathrm{CO_2}$, $\mathrm{H_2}$, $\mathrm{H_2O}$, $\mathrm{CH_4}$, C, $\mathrm{N_2}$ and $\mathrm{SO_2}$, while $Sr_{j,i}$ and $Sp_{j,i}$ are the stoichiometric coefficients of the stoichiometric coefficients matrix for the reactants $[Sr]$ and the stoichiometric coefficients matrix for the products $[Sp]$, respectively. The subscripts i and j correspond to the individual species and reactions, so that the stoichiometric coefficient matrices for the reactants and products can be expressed as

$$[Sr] = \begin{bmatrix} 1 & 0 & 0 & 1 & 0 & 0 & 0 & 0 \\ 0 & 0 & 0 & 1 & 1 & 0 & 0 & 0 \\ 0 & 1 & 0 & 0 & 0 & 1 & 0 & 0 \\ 0 & 0 & 0 & 1 & 0 & 1 & 0 & 0 \\ 0 & 0 & 2 & 0 & 0 & 1 & 0 & 0 \end{bmatrix} \tag{5}$$

$$[Sp] = \begin{bmatrix} 0 & 1 & 1 & 0 & 0 & 0 & 0 & 0 \\ 1 & 0 & 3 & 0 & 0 & 0 & 0 & 0 \\ 2 & 0 & 0 & 0 & 0 & 0 & 0 & 0 \\ 1 & 0 & 1 & 0 & 0 & 0 & 0 & 0 \\ 0 & 0 & 0 & 0 & 1 & 0 & 0 & 0 \end{bmatrix} \tag{6}$$

As the degree of advancement for each reaction changes due to thermochemical conversion, the concentrations of reactants and products can be related in terms of the stoichiometric coefficient as

$$\dot{n}f_i = \dot{n}_i + \sum_{j=1}^{R_n} \left[\in_j \left(Sp_{j,i} - Sr_{j,i}\right)\right] \tag{7}$$

The total gaseous flow rate (excluding the char) through the system can be written as

$$\dot{n}_{\mathrm{totmol}} = \sum_{i=1(i\neq 7)}^{\mathrm{ns}} \dot{n}f_i \tag{8}$$

The relation between the fractional concentration of each species (χ_i) and the equilibrium constant (K_{eq}) for each chemical reactions is established using the statement of chemical equilibrium at constant temperature and pressure [14] as

$$\prod_{i=1}^{i=\mathrm{ns}} (\chi_i P)^{Sp_{j,i}} - K_{\mathrm{eq},j} \prod_{i=1}^{i=\mathrm{ns}} (\chi_i P)^{Sr_{j,i}} = 0; \quad \text{for } j = 1, 2, \ldots R_{\mathrm{n}} \tag{9}$$

The fraction of concentration of the ith species of the system then can be written as

$$\chi_i = \frac{\dot{n}f_i}{\dot{n}_{\mathrm{totmol}}} \tag{10}$$

The equilibrium constants needed for the present work are obtained using the arguments of the natural logarithm in terms of the Gibbs function for each constituent and the stoichiometric coefficients for the reactants and products, respectively, as

$$K_{\mathrm{eq},j} = \mathrm{e}^{-\left(\sum_{i=1}^{\mathrm{ns}} Sp_{j,i}\frac{g_i^0(T)}{RT} - \sum_{i=1}^{\mathrm{ns}} Sr_{j,i}\frac{g_i^0(T)}{RT}\right)} \tag{11}$$

R in the above expressions stands for the universal gas constant.

The Gibbs function for the ith species, has been obtained using the NASA polynomial for the data of the JANAF thermochemical tables available in the literature [15] as given by

$$\frac{\bar{g}_i^o(T)}{R_u T} = Ag_i + Bg_i T + Cg_i T^2 + Dg_i T^3 + Eg_i T^4 + \frac{Fg_i}{T} + Gg_i \ln T \tag{12}$$

Here, i denotes the species present in the system, and the values of constants Ag_i to Gg_i for the ith components are well documented in Sharma [15].

3.3. Modeling energy equation

The energy equation has been modeled to predict the char bed temperature. It accounts for the heat inflows and outflows in the control volume due to fluid and fuel flows, the heat loss to the surroundings, conduction and radiation heat transfer between adjacent control volumes and the quantity of heat consumed in a control volume as shown in Fig. 2. Thus, the energy equation can be written as

$$\sum_{\mathrm{react}} \dot{m}_i h_i + \left(-k_{\mathrm{eff}} A \nabla T\right)_{\mathrm{in}} - \dot{Q}_{\mathrm{loss}} + \dot{Q}_{\mathrm{reac}} = \sum_{\mathrm{prod}} \dot{m}_i h_i + \left(-k_{\mathrm{eff}} A \nabla T\right)_{\mathrm{out}} \tag{13}$$

$$h_i = \int_{T_A}^{T} Cp_i \mathrm{d}T \tag{14}$$

Here, h_i is the sensible enthalpy change with respect to the surroundings, it is comprised of the char and combustion products at various stage of the reduction process. The subscripts react and prod denote the reactants and combustion products. K_{eff} is the effective thermal conductivity of the char bed filled with gas mixture. The model of Sharma [16] has been employed to calculate the K_{eff} of the porous char bed in terms of bed temperature, particle size and bed porosity. $\dot{Q}_{\mathrm{loss}}$ is heat loss to the surroundings (Fig. 2).

$\dot{Q}_{\mathrm{reac}}$ denotes the endothermic heat released in the char reduction zone. As the reactions (R1–R5) proceed, the

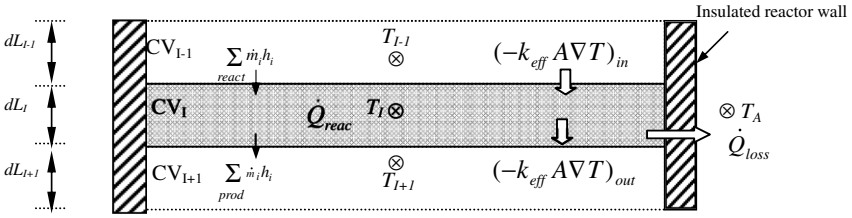

Fig. 2. Sketch of a single control volume used for heat transfer analysis.

reaction temperature in the bed decreases due to the endothermic nature of the heterogeneous reactions of the char and gaseous products of the combustion reaction. The heat absorption in the char reduction zone, thus, can be determined using the enthalpy of formation of the reactants and products as given by

$$\dot{Q}_{\text{reac}} = \sum_{\text{react}} \dot{m}_i h^0_{f,i} - \sum_{\text{prod}} \dot{m}_i h^0_{f,i} \tag{15}$$

Here, the heat of formation of each constitutent can be directly known [14].

Once, the initial concentration of the reactants in the reduction reaction is known (Eq. (1)), the chemical equilibrium Eq. (9) for each global reduction reactions, in conjunction with Eqs. (7), (8) and (10) along with the equilibrium constant Eq. (11), form a set of equations, which are solved for the degree of advancement for each chemical reaction at the prescribed value of reaction temperature for initialization. This gives the concentrations of each product of the system. During parametric studies, it is seen that under extreme operating conditions (i.e. at high reaction temperature), the char yield turns negative. Thus, in the present work, when the char becomes less than zero, it is assigned as zero, and the heterogeneous char–gas reactions (R3–R5) have been dropped in the full equilibrium calculations and the remaining equations for the homogeneous reactions (R1–R2) are solved using Newton's method of convergence [14] in order to predict the species concentration in the reduction zone.

Once concentrations of the reduction reaction products are known, the energy Eq. (13), followed by the equation for the heat of absorption Eq. (15), is used to modify the initial guess for the reaction temperature. Iterations are performed until convergence.

4. Property data

The specific heat (kJ/kg K) and thermal conductivity (W/m K) of the char as a function of specific gravity (Sg_{char}) is known from Ragland et al. [17].

$$C_{p_{\text{char}}} = 1.39 + 0.00036T \tag{16}$$

$$K_{\text{char}} = 0.67 Sg_{\text{char}} - 0.071 \tag{17}$$

The specific heats and thermal conductivity of the gas mixture then can be obtained as [18]

$$C_{p_{\text{gas-mixture}}} = \sum\nolimits_{\text{gases}} Y_i Cp_i \tag{18}$$

$$k_{\text{gas-mixture}} = \frac{\sum_{i=1}^{i} \chi_i k_i (mw_i)^{0.333}}{\sum_{i=1}^{i} \chi_i (mw_i)^{0.333}} \tag{19}$$

For each species, the polynomial equation fit of Thunman et al. [19] for specific heat and the cubic polynomial curve fit of Reid et al. [20] for thermal conductivity have been used in the present work. The representative curve fit equations are given as

$$C_{p_i} = a_i + b_i T + c_i T^2 + d_i T^3 + e_i T^4 \tag{20}$$

$$k_i = A_i + B_i T + C_i T^2 + D_i T^3 \tag{21}$$

The values of the constants are known from their respective references.

5. Simulation results and discussion

The equilibrium model developed above has been used to predict the gas composition, unconverted char, calorific value of gas, gasification efficiency and endothermic heat released in the char reduction zone for known biomass composition, equivalence ratio, initial reactant temperature and pressure.

5.1. Validation of the model

The predictions of the equilibrium model developed above have been compared for 'equilibrium constants of global reactions' and for 'composition of producer gas' against data collected from various sources for downdraft biomass gasifiers. The equilibrium constants of the global reactions describing the char–gas and gas–gas reactions in the reduction zone are compared with previously published tabulated data of Reed and Markson [11] for the most likely temperature range in the reduction zone as shown in Fig. 3. The equilibrium constants of the steam reformation reaction (R1), Boudourd reaction (R3) and water–gas (primary) reaction (R4) increase steeply at the higher reaction temperatures, while the methanation reaction (R5) and water–gas shift reaction (R2) both show decreasing trends. The predictions of equilibrium constants are in good agreement with the tabulated data of Reed and Markson [11].

Equilibrium model predictions for the dry gas composition and calorific value of the gas have been tested against

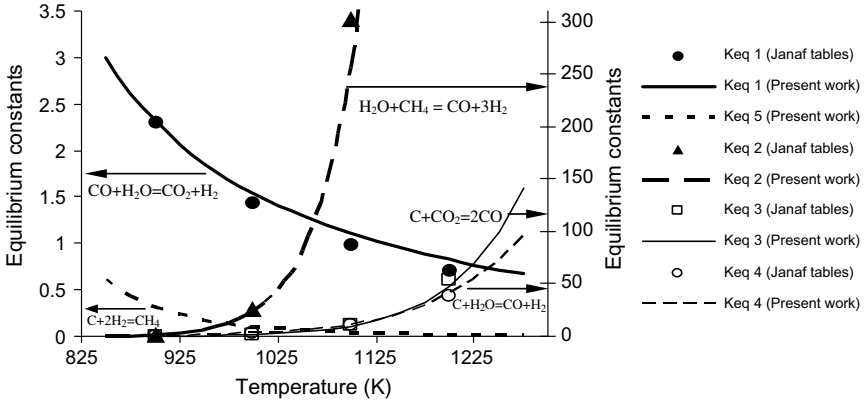

Fig. 3. Comparison of predicted and data calculated from JANAF tables for thermodynamic equilibriums constants of reduction reactions against temperature.

the experimental data of Chee [21], Senelwa [22] and data predicted by the kinetic model of Giltrap et al. [2] for Douglas fir bark with ultimate analysis of 56.2% C, 5.9% H, 36.7% O and higher heating value 22097 kJ/kg [10]. Table 1 shows the parameters used in the comparison.

Comparing the predicted values with the experimental data of Chee [21] and Senelwa [22] and with the predicted data of the kinetic model [2], it is observed that for hydrogen, the proposed equilibrium model shows slight over predictions, while for carbon monoxide and methane; it gives slight under predictions as shown in Fig. 4. The under prediction of CH_4 is expected for all equilibrium models, since the equilibrium constant for the methanation reactions tends to zero, while for the steam reforming reaction it tends to infinity at the elevated temperatures prevailing in the reduction zone (Fig. 3). As a result, the predicted CH_4 concentration in the final gas is small. Even though the model predictions for calorific value agree well with both experimental data, the predicted data of the kinetic model [2] deviates significantly. The present model shows reasonable agreement for the dry gas composition and fairly good agreement for the calorific value of the gas in comparison with the above experimental data.

Table 1
Parameters used in experimental downdraft biomass gasification and in the model simulation

Parameter	Chee [21] data	Senelwa [22] data	Giltrap et al. [2]	Present model
Bed length	Not stated	0.275 m	0.275 m	0.275 m
T initial	Not stated	1228 K	1200 K	1228 K
Biomass	Cotton wood chip	–	Douglas for bark	Douglas fir bark
Moisture content	5.4 wt% (wet basis)	'Oven dried'	0	5 wt%
Equivalence ratio (air/feed ratio)	(1.67) calculated	–	–	0.4

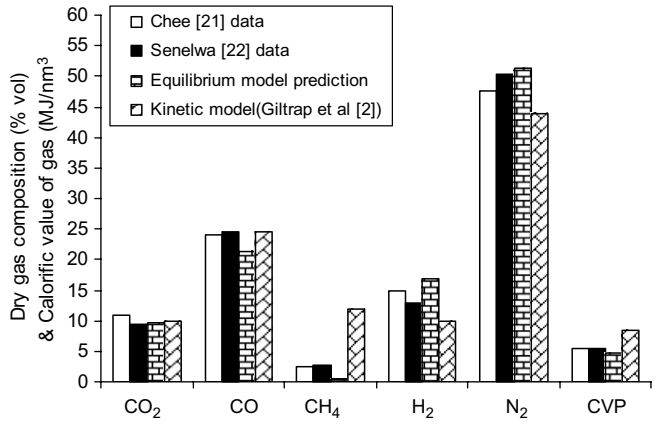

Fig. 4. Comparison of predicted and data reported in the literature for dry gas composition and calorific value of gas.

5.2. Parametric studies

Once the model has been validated, the roles of moisture content in the feedstock, pressure, equivalence ratio and initial reaction temperature in the reduction zone on the dry gas composition, unconverted char, calorific value, gasification efficiency, heat absorbed in the reduction zone and outlet gas temperature have been examined. Douglas fir bark as feedstock, having a typical moisture content of 12% (dry basis) at the typical equivalence ratio of 0.39 (=ratio of actual air flow to stoichiometric requirement of air flow) has been considered as baseline values for the present parametric studies.

5.2.1. Moisture content

The effects of moisture content (dry basis) in a typical biomass, 'Douglas fir bark', have been studied on the dry gas composition, unconverted char, calorific value of gas, gasification efficiency, outlet gas temperature and heat absorbed in the reduction zone as shown in Figs. 5–7. In Fig. 5, the results on the dry gas composition and unconverted char are presented. It is seen that with an increase in moisture content in the feedstock, the CO percentage in the dry gas decreases, while the H_2 and CO_2 percentages

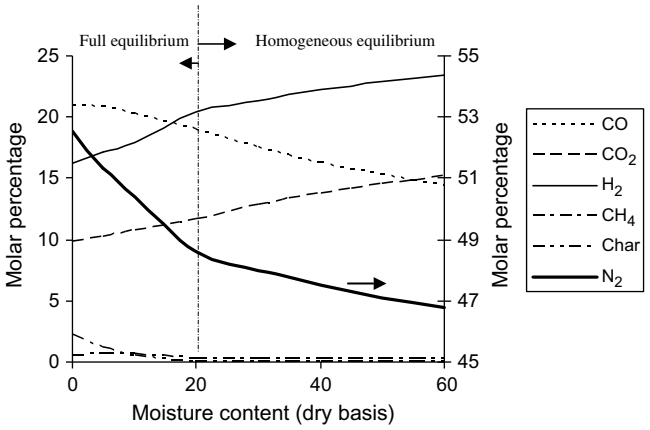

Fig. 5. Effect of moisture content in biomass on dry gas composition and unconverted char.

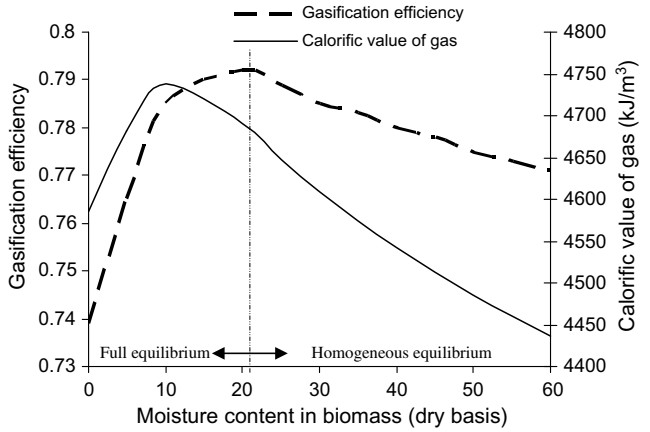

Fig. 6. Effect of moisture content in biomass on dry gas composition and unconverted char.

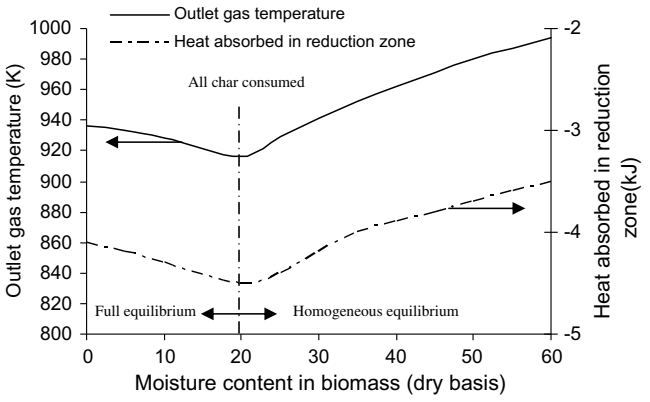

Fig. 7. Effect of moisture content in biomass on outlet gas temperature and heat absorbed in reduction zone.

grow. The growth of H_2 is sharp until all char gets consumed (beyond which the full equilibrium model predicts a negative value of char, which is forced to zero using the homogeneous equilibrium model), after which the growth is not sharp (see RHS Fig. 5). Increasing the moisture in Douglas fir bark shows similar trends for CO_2. It can be observed from a close scrutiny of Fig. 5 that the percentage of CO decreases slightly up to ~10% moisture addition, and thereafter, it starts reducing sharply for further addition of moisture in the feedstock. The predicted percentage of methane is quite low and does not show any considerable role with variation in moisture level in the feedstock. In Fig. 6, the calorific value and gasification efficiency are plotted against the moisture content. The trend for the calorific value of the gas shows improvement with the increase in moisture content from 0% to 10%, with a maximum value of 4738 kJ/m^3 at 10% moisture, thereafter, it starts decreasing with further increase in moisture content. The gasification efficiency also shows similar trends. However, it must be noted that the gasification efficiency shows a peak near 20% moisture content when all char gets consumed.

The effect on outlet gas temperature and heat absorbed in the reduction zone has been illustrated in Fig. 7. The predictions show that the endothermic behavior (i.e. heat absorption in the bed) grows with moisture content, which tends to decrease the reaction temperature and, hence, the outlet gas temperature decreases until all char gets converted into gaseous products due to these heterogeneous reduction reactions, beyond which homogeneous equilibria is established and thus diluting the endothermic behaviour of the system resulting the reaction temperature and the outlet gas temperature starts increasing in the reduction zone (Fig. 7).

The peaking of calorific value even before the condition of all char conversion, is understandable, since the steep fall of CO percentage can be observed beyond 10% addition of moisture, resulting in a sharp decrease in calorific value of the gas. However, the peak in gasification efficiency at 20% moisture content is quite obvious, since the gas quantity increases as more char gets converted into gaseous product, which is the main cause of increasing the gasification efficiency. Likewise, as more char converts into gas, the reduction zone will show more endothermic behaviour and, thus, lead to a decrease in the outlet gas temperature.

5.2.2. Pressure

The role of increased pressure has been investigated on the equilibrium percentage of various species in the dry gas, unconverted char, calorific value of the gas, gasification efficiency, outlet gas temperature and heat absorbed in reduction zone as shown in Figs. 8–10. Fig. 8 gives the equilibrium percentages of the dry gas species and unconverted char in the reduction zone as a function of gasifier pressure. It follows that the percentages of CO and H_2 decrease as the pressure increases, as expected from Chatelier's principle, while the CH_4, CO_2, N_2 and unconverted char grow with increasing pressure.

Fig. 9 shows the effect of pressure on the predicted calorific value of the gas and the gasification efficiency. The calorific value of the gas decreases as pressure increases, since the percentages of hydrogen and carbon monoxide decrease significantly, as compared to the improvement in

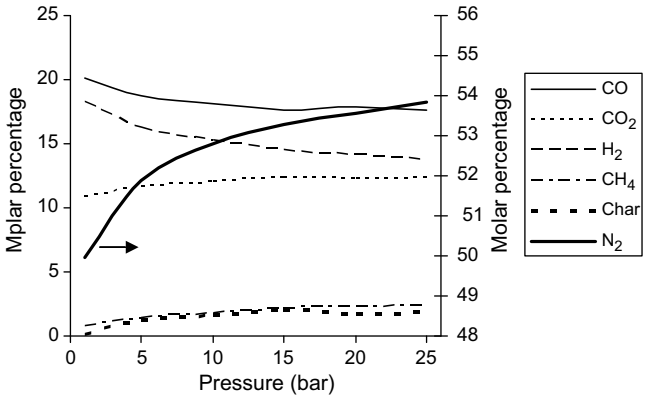

Fig. 8. Effect of pressure on dry gas composition and unconverted char, full equilibrium.

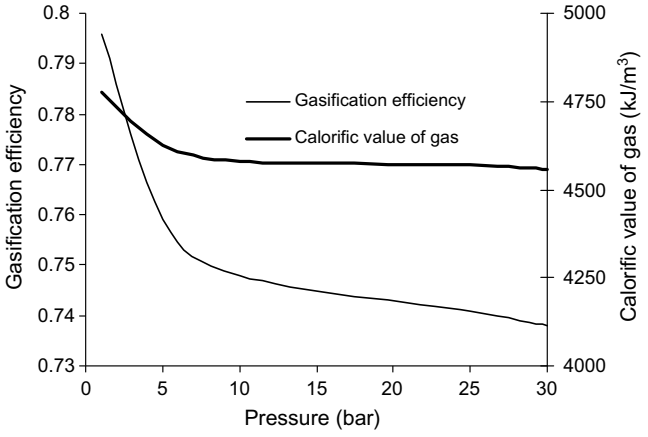

Fig. 9. Effect of pressure on gasification efficiency and calorific value of gas, full equilibrium.

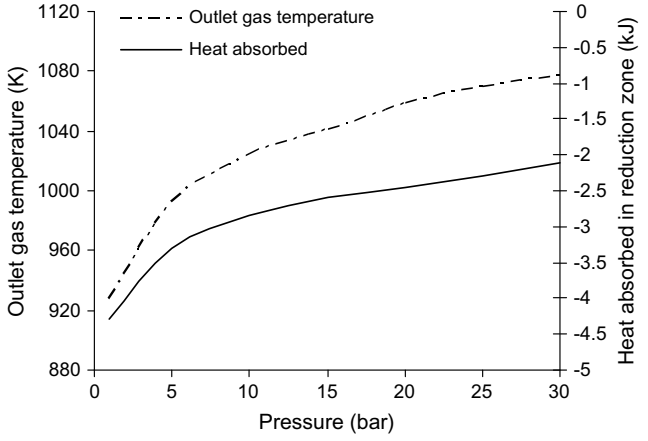

Fig. 10. Effect of pressure on outlet gas temperature and heat absorbed in reduction zone; full equilibrium.

the percentage of methane with increasing pressure. Similarly, the gasification efficiency also decreases with an increase in pressure. It is to be noted that the pressure has a significant influence over a limited pressure range (about 1–7 bar). Beyond this range, the influence of pressure is not so significant on the calorific value of the gas and the gasification efficiency.

The fate of the heat absorbed in the reduction zone and the outlet gas temperature has been predicted in Fig. 10. The endothermic behaviour (or heat absorbed in the reduction zone) dilutes with increase in pressure. This dilution of the endothermic nature is expected since all the heterogeneous reactions responsible for conversion of char into gaseous product reverse at higher pressures, as expected from Chatelier's principle and thus, the outlet gas temperature of the reaction zone starts increasing with increased pressure.

5.2.3. Equivalence ratio (gasification)

The effects of equivalence ratio in the gasifier have been investigated on the dry gas composition, unconverted char, calorific value of gas, gasification efficiency, outlet gas temperature and endothermic heat released in the reduction zone as shown in Figs. 11–14. In Fig. 11, the dry gas composition has been plotted against equivalence ratio (gasification). The percentages of H_2, CO and unconverted char decrease with increase in equivalence ratio, while the percentages of CO_2 and N_2 grow with increase in equivalence ratio for both the full equilibrium and homogeneous equilibrium calculations.

Since, the calorific value of the final gas and the gasification efficiency are found to be sensitive to the equivalence ratio and moisture content in the feedstock, more predictions are plotted for detained analysis for the most likely operating conditions of moisture content (i.e. 12%, 16% and 20%) prevailing in a downdraft biomass gasifier. In Fig. 12, the predictions of calorific value of the final gas are given. It is seen that the calorific value of the final gas decreases monotonically with increasing equivalence ratio. The results also show that for increasing moisture content, the calorific value of the gas improves at lower equivalence ratios, while at higher equivalence ratios, the calorific value of the gas decreases slightly.

Fig. 13 illustrates the effect of equivalence ratio on gasification efficiency for different moisture contents in the feedstock. From the predictions, a peak in gasification efficiency can be observed. This peak of gasification efficiency

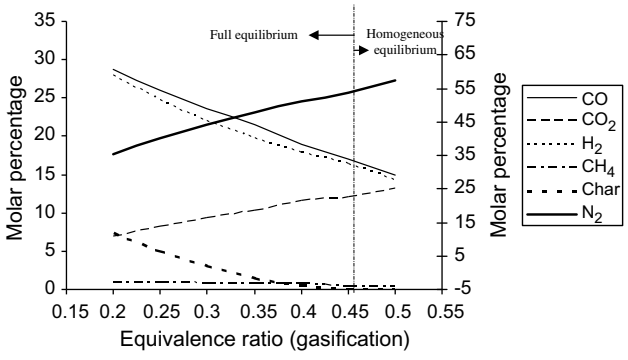

Fig. 11. Effect of equivalence ratio (gasification) on dry gas composition and unconverted char.

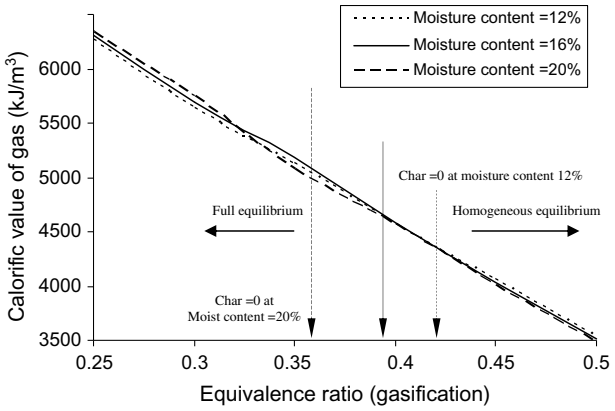

Fig. 12. Effect of equivalence ratio (gasification) on calorific value of gas.

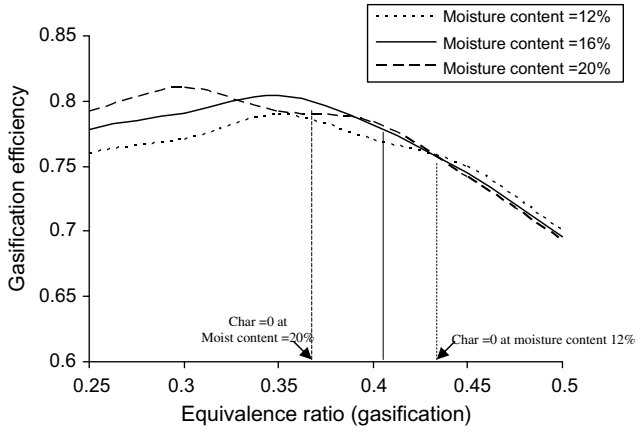

Fig. 13. Effect of equivalence ratio (gasification) on gasification efficiency.

shifts toward lower equivalence ratio with the addition of moisture content in the feedstock. It must be noted that the condition of total char consumption is reached some what earlier in the case of higher moisture content as compared to the case of the feedstock having less moisture content.

The effects on outlet gas temperature and heat absorbed in the reduction zone have been plotted in Fig. 14. The heat absorbed in the reduction zone, or endothermic nature, dominates until all char gets consumed in the reduction zone, which leads to increase in the reaction temperature and, thus, outlet gas temperature. Thereafter, the endothermic behavior starts decreasing (since there is no more char available in the system to convert), and hence, the outlet gas temperature starts increasing for further increase in equivalence ratio or inlet air (Fig. 14).

5.2.4. Initial temperature in reduction zone

The effects of initial temperature in the reduction zone have been examined on the dry gas composition, unconverted char, calorific value of gas, gasification efficiency, outlet gas temperature and heat absorbed in reduction zone as shown in Figs. 15–17. Fig. 15 shows the CO percentage in the gas grows more sharply than the hydrogen percentage for the initial increase in inlet temperature until all the char gets converted into gases.

Thereafter, the homogeneous equilibria show some improvement in CO, while H_2 does not show any significant variation for further increase in initial temperature. Similarly, the prediction of methane does not reflect any significant variation with initial temperature.

The calorific value and gasification efficiency are plotted against the initial temperature as shown in Fig. 16. It is observed that the calorific value of the gas and the gasification efficiency both increase from 1100 to ~1225 °C, where all the char gets consumed, and thereafter, this increase is not significant for either parameter with further increase in initial temperature.

Fig. 17 shows the roles of initial temperature on the outlet gas temperature and heat absorbed in the reduction zone. Initially, as char is available for reaction, the temperature of the outlet gas improves gently due to domination of the endothermic reactions. Thereafter, as no more char is left, the endothermic behavior is diluted, and thus, the temperature of the outlet gas tends to rise sharply.

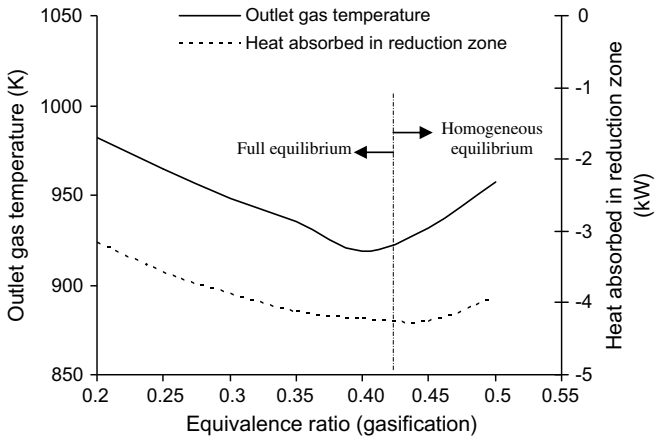

Fig. 14. Effect of equivalence ratio (gasification) on outlet gas temperature and heat absorbed in reduction zone.

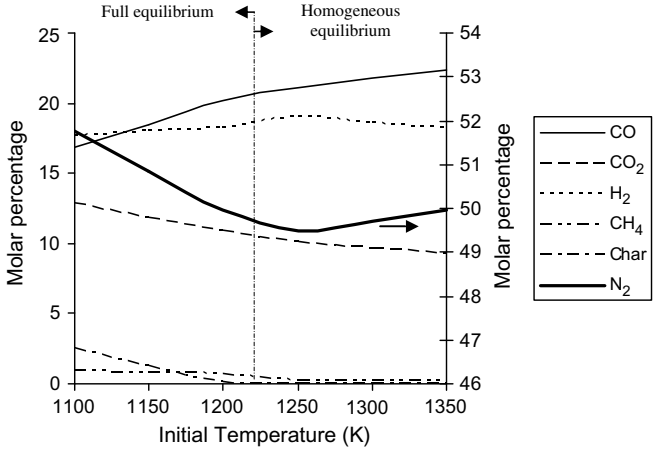

Fig. 15. Effect of initial gas temperature on dry gas composition and unconverted char.

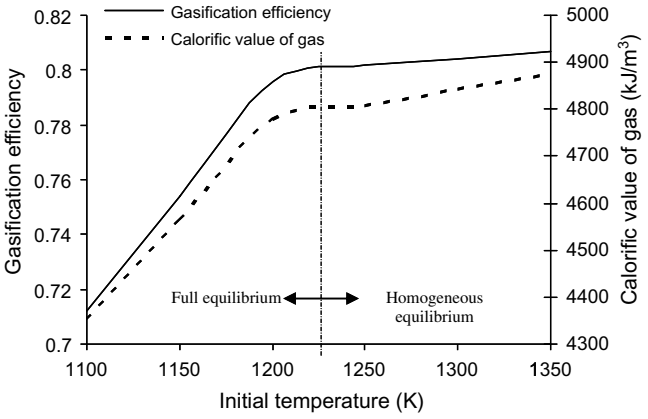

Fig. 16. Effect of initial temperature on gasification efficiency and calorific value of gas.

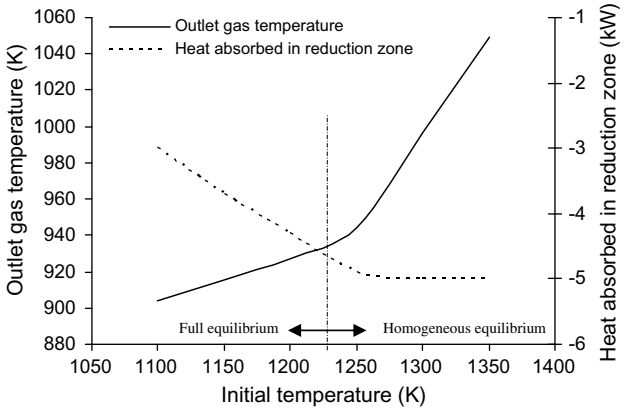

Fig. 17. Effect of initial temperature on outlet gas temperature and heat absorbed in reduction zone.

In the present work, the correlation of Chen and Gunkel [23] for bed porosity has been used. The average particle diameter of 3 cm has been considered, which reduces to ash of particle size 3 mm. Typical results show the dry gas composition (i.e. excluding the H_2O), as the dry product gas is of interest to most researchers.

6. Conclusions

A detailed equilibrium model for global reduction reactions describing the char–gas and gas–gas reactions in the char reduction zone of a downdraft biomass gasifier has been presented. The accurate reaction temperature in the char bed has been computed by modeling the energy equation for the thermal interaction of neighboring zones and heat loss to the surroundings using the effective thermal conductivity approach. Model predictions for equilibrium constants and dry gas composition have been validated by comparing the data collected from various sources. The comparison of model simulation results shows reasonably good agreement with these data.

Simulations modeling the influence of various operating parameters of the gasifier for Douglas fir bark, such as (1) moisture content in feedstock, (2) pressure, (3) equivalence ratio and (4) initial temperature on the dry gas composition, unconverted char, calorific value of gas, gasification efficiency, outlet gas temperature and endothermic heat released in the reduction reaction zone. The condition of complete char conversion has been investigated. It is also found that the condition of complete char conversion shifts toward lower equivalence ratio for the case of feedstock having higher moisture content. For optimal energy conversion of Douglas fir bark, the range of various parameters should be limited to 10–20% (dry basis) for moisture content and 0.3–0.45 for equivalence ratio, while the initial temperature in the reduction reaction zone should not be less than 1200 K. However, the maximum temperature limit can be decided on the basis of ash fusion temperature for the typical class of wood. The role of pressure is found to be quite unfavorable in all conditions under investigation.

The proposed equilibrium model for the reduction zone can predict full equilibrium composition and equilibrium constants precisely and, thus, can be used as a reduction reaction module for computer simulation of downdraft gasifier systems. Equilibrium models are also important and useful in predicting the highest thermal or gasification efficiency that can possibly be attained for a given feedstock.

References

[1] Wang Y, Kinoshita CM. Kinetic model of biomass gasification. Sol Energy 1993;51(1):19–25.
[2] Giltrap DL, McKibbin R, Barnes GRG. A steady state model of gas–char reactions in a downdraft gasifier. Sol Energy 2003;74:85–91.
[3] Babu BV, Sheth PN. Modeling and simulation of reduction zone of downdraft biomass gasifier: effect of char reactivity factor. Energy Convers Manage 2006;47(15–16):2602–11.
[4] Buekens AG, Schoeters JG. Modelling of biomass gasification. In: Overend RP, Milne TA, Mudge LK, editors. Fundamental of thermochemical biomass conversion. Elsevier Applied Science; 1985. p. 619–89.
[5] Ruggiero M, Manfrida G. An equilibrium model for biomass gasification processes. Renew energy 1999;16:1106–9.
[6] Zainal ZA, Ali R, Lean CH, Seetharamu KN. Prediction of performance of a downdraft gasifier using equilibrium modeling for different biomass materials. Energy Convers Manage 2001;42:1499–515.
[7] Altafini CR, Wander PR, Barretoa RM. Prediction of the working parameters of a wood waste gasifier through an equilibrium model. Energy Convers Manage 2003;44(17):2763–77.
[8] Malgar A, Pérez JF, Laget H, Horillo A. Thermochemical equilibrium modelling of a gasifying process. Energy Convers Manage 2007;48(1):59–67.
[9] Prins MJ, Ptasinski KJ, Janseen FJJG. From coal to biomass gasification: comparison of thermodynamic efficiency. Energy 2007;32(7):1248–59.
[10] Graboski M, Bain R. Properties of biomass relevant to gasification, vol. 16. New Jersey: Noyes Data Corporation; 1981. p. 41–71.
[11] Reed TB, Markson M. A predictive model for stratified downdraft gasifier. In: David A. Tillman, Edwin C. John, editors. Solar Energy Research Institute Golden. Colorado; Progress in Biomass Conversion, vol. 4; 1983, p. 219–54.

[12] Grover PD, Baveja KK, Rao TR, Iyer PVR. Thermochemiocal characterisation of biomass residues for gasification, vol. I, Biomass Research Laboratory. IIT Delhi; 1988.
[13] Shafizadeh F. Pyrolytic reactions and products of biomass. J Anal Appl Pyrol 1982;3:283–305.
[14] Turns SR. Introduction to combustion. 2nd ed. McGraw Hill; 2000.
[15] Sharma Avdhesh Kr. Simulation of a biomass gasifier-engine system 2006; Ph.D. Thesis, Mechanical Enginering Deparment, Indian Institute of Technology, Delhi, India.
[16] Sharma Avdhesh Kr. IMECE2005-80758: Modeling conduction and radiation in the reactive, porous bed of the gasifier 2005. In: Proceedings of 2005 ASME international mechanical engineering congress and exposition. November 5–11. Orlando, Florida, USA.
[17] Ragland KW, Arts DJ, Baker AJ. Properties of wood for combustion analysis. Bioresour Technol 1991;37:161–8.
[18] Perry RH, Green DW. Perry's chemical engineers handbook 1998; 7th MGH International edition, NY.
[19] Thunman H, Niklasson Johnson F, Leckner B. Composition of volatile gases and thermochemical properties of wood for modelling of fixed or fluidized beds. Energy Fuel 2001;15:1488–97.
[20] Reid RC, Prausnitz JM, Poling BE. The properties of gases and liquids. 4th International edition. NY: McGraw-Hill Company; 1988.
[21] Chee CS. The air gasification of wood chips in a downdraft gasifier. MSc thesis. Kansas University; 1987.
[22] Senelwa K. The air gasification of woody biomass from short rotation forests. Ph.D. Thesis. Massey University New Zealand; 1997.
[23] Chen JS, Gunkel WW. Modeling & simulation of cocurrent moving bed gasification reactors-part I, a non-isothermal particle model. Biomass 1987;14(1):51–72.